applied sciences

MDPI

Article

Performance Evaluation of Steel Slag Asphalt Mixtures for Sustainable Road Pavement Rehabilitation

José Neves [1,*] and João Crucho [2]

[1] CERIS, Department of Civil Engineering, Architecture and Georesources, Instituto Superior Técnico, Universidade de Lisboa, Avenida Rovisco Pais, 1049-001 Lisbon, Portugal
[2] CERIS, Instituto Superior Técnico, Universidade de Lisboa, Avenida Rovisco Pais, 1049-001 Lisbon, Portugal; joao.crucho@tecnico.ulisboa.pt
* Correspondence: jose.manuel.neves@tecnico.ulisboa.pt

Abstract: The demand for more sustainable transport infrastructure has led to a broader acceptance of waste materials in pavements. An excellent example of this trend is the incorporation of steel slag aggregates (SSA) in asphalt mixtures. This work evaluates the mechanical performance of asphalt mixtures that include SSA in their composition. Asphalt mixtures were evaluated through laboratory tests for affinity between binder and aggregate, Marshall and volumetric properties, stiffness, resistance to fatigue, permanent deformation, and water sensitivity. Two rates of SSA incorporation—20% and 35%—were considered. In general, results indicated that incorporating SSA has not impaired the behavior of the asphalt mixtures. In some cases, the presence of SSA has improved mechanical performance. It was the case of the resistance to permanent deformation, stability, flow, and water sensitivity. This work confirms the suitability of the SSA application in asphalt mixtures beyond the benefit of promoting industrial waste in pavement engineering.

Keywords: asphalt mixtures; mechanical behavior; pavement rehabilitation; steel slag

Citation: Neves, J.; Crucho, J. Performance Evaluation of Steel Slag Asphalt Mixtures for Sustainable Road Pavement Rehabilitation. *Appl. Sci.* **2023**, *13*, 5716. https://doi.org/10.3390/app13095716

Academic Editor: Cesare Oliviero Rossi

Received: 14 March 2023
Revised: 24 April 2023
Accepted: 2 May 2023
Published: 5 May 2023

1. Introduction

The need to accelerate the convergence to the 2030 Agenda for Sustainable Development Goals (SDG), adopted by the United Nations Member States in 2015, is becoming increasingly urgent. Numerous technological innovations have emerged from research in recent years, contributing to a circular economy and more sustainable and resilient human activity. Moving from theory to practice is crucial. Simple and easy-to-implement technologies should be promoted. Transport infrastructures (e.g., roads, railways, airfields, pipelines) are essential for the development of society and must contribute to the SDG. To maintain the quality of infrastructures, every year, resources are consumed on a large scale worldwide in construction and maintenance actions. Using waste materials in transport infrastructure applications is a promising and efficient strategy [1,2].

Waste generation is a global environmental problem, and the steel industry is one of the critical contributors to this negative impact. In addition to moving a large volume of raw materials and consuming energy, it also generates large amounts of solid waste, such as slags. The steel industry produces two main types of slag: Blast Furnace Slag (BFS) and Steel Furnace Slag (SFS). The total production of BFS from SFS in 2018 in Europe was 20.7 and 16.3 million tons, respectively, according to the latest production survey carried out by Euroslag, the European association representing producers and processors of metallurgical slag [3].

Nowadays, the disposal of this waste in landfills is not feasible due to the high volumes being generated, the high costs involved, and the environmental inconvenience it entails. Thus, several alternative solutions are being studied to enhance these by-products for other applications, promoting the environmental sustainability of this material. The construction and rehabilitation of road pavements is a significant consumer of aggregates, not only for non-bonded sub-base and base layers but also for asphalt or hydraulic mixes. To promote more sustainable solutions, pavement engineering has been using new alternative materials to reduce the consumption of non-renewable natural resources. In the case of SFS, 70.6% of production in 2018 has already been used in road construction in Europe [3]. In the USA, 7.7 to 8.3 million tons of steel slag is used annually, mostly in granular bases or as a construction material [4].

Besides physical and mechanical properties, complementary studies related to expansibility and environmental evaluation should be addressed when dealing with non-traditional materials to prove their adequacy for construction purposes. In the case of steel slag, one of the main concerns is the propensity for expansion, which can cause detrimental damage to materials. In Portugal, electrical arc furnace steel slag is submitted to maturation periods to become an inert material. After this process, SSA acquires the CE marking as an aggregate for use in civil engineering work and road construction according to EN 13242 [5]. In this work, the SSA used in the experimental program was previously submitted to leaching tests, which confirmed that it behaves as an inert aggregate [6].

The feasibility of using steel slag aggregates (SSA) in asphalt mixtures, substituting natural aggregates, has been extensively conducted in the literature concerning mechanical and environmental aspects [7–9]. Two main perspectives for the use of SSA can be achieved: a perspective of promoting sustainability through the reduction of the consumption of natural resources (substitution of natural aggregates) [10,11]; and a more ambitious perspective related to the promotion of multifunctional pavements by inducing self-healing or self-sensitive properties of the asphalt mixtures [12–14].

Several authors have confirmed that incorporating SSA into asphalt mixtures did not impair pavement performance. Studies of the literature showed the benefits of using SSA considering various factors, such as the type of asphalt mixture, origin of natural or recycled aggregate, grading, and function of SSA [15–22]. Several mechanical and functional properties were analyzed (e.g., cracking, moisture damage, rutting, skid resistance) that confirmed the acceptable performance of the asphalt mixtures with SSA [23–29].

Regarding the use of SSA in asphalt mixtures, most studies in the literature have considered a selected grading (crushed steel slag fine or coarse aggregates). Such an approach can be laborious or challenging to implement in the case of actual conditions of production and pavement application. In Europe, SSA is produced under Factory Production Control, and it should be in conformity with the marking requirements of the Construction Products Regulation. In Portugal, SSA is available through different aggregate dimensions, and the most common is 0/40 all-in aggregate. The innovation of this work is related to the SSA incorporation method: two fractions of aggregate dimension 0/20 of natural aggregates and SSA were simply mixed in different percentages: 0%, 20%, and 35% of SSA. In this process, there was no need to make a previous and complex grading selection of the aggregates, therefore easing its implementation in the production of asphalt mixtures. The percentages of SSA incorporation were selected by considering the existing literature and earlier work from the authors [25]. The use of high ratios of SSA incorporation is not recommended. Due to the high density of the SSA, approximately 1 Mg/m^3 higher than that of a natural aggregate [30,31], high incorporation rates may limit the volume carried by trucks increasing the transportation costs.

This paper analyzes and discusses the mechanical performance of the asphalt mixtures containing SSA (0%, 20% and 35%) evaluated through the following laboratory tests: affinity between binder and aggregate, Marshall and volumetric properties, stiffness, resistance to permanent deformation, fatigue resistance, and water sensitivity. The results of this work are intended to be a valuable contribution towards achieving the Sustainable Development Goals adopted by the United Nations on transport infrastructure [1].

2. Materials and Methods

2.1. Materials and Specimen Preparation

Natural aggregates, SSA, mineral filler, and bituminous binder were used to produce the asphalt mixtures. The selected mixture type was—AC 20 base 35/50—an asphalt concrete for the base layer, with a maximum aggregate size of 20 mm and using as binder a bitumen with penetration class 35/50. The penetration class 35/50 was selected because this is the most used in Portuguese paving technology and other regions with similar climatic conditions. The same filler, from limestone origin, and paving grade bitumen were used throughout the study. In this manner, these materials were not a variable.

The natural aggregate (NA) selected to produce the asphalt mixtures was obtained from crushed limestone rock produced by a local quarry. The SSA was obtained from a steel production plant. In this plant, SSA is generated by the electric arc furnace (EAF) and the factory production control is certified according to the requirements set by EN 13242:2002+A1:2007 [5]. Table 1 presents the mechanical and physical properties of the NA and SSA. In this study, the same fraction—0/20—was considered for both aggregates.

Table 1. Mechanical and physical properties of the aggregates.

Property	NA	SSA
Apparent particle density (Mg/m^3)	2.694	3.689
Particle density on an oven-dried basis (Mg/m^3)	2.619	3.530
Particle density on a saturated and surface-dried basis of aggregate (Mg/m^3)	2.647	3.573
Water absorption (%)	1.1	1.2
Resistance to fragmentation by the Los Angeles test method (LA)	30	25
Methylene blue (g/kg)	1.0	0.2
Sand equivalent (SE)	39	78
Flakiness index (FI)	11	1
Shape index (SI)	10	2

The formulation of the asphalt mixture was done according to the Marshall method. The optimum binder content, 4.7%, was determined for the reference mixture (0% SSA) and then reproduced in the mixture with 20% SSA. Due to the high density of the SSA, maintaining the same binder content in % by mass of mixture would lead to a higher volumetric quantity of binder. Thus, for the mixture with 35% SSA was applied the same binder content in % by volume, equal to the mixture with 20% SSA. The composition of the asphalt mixtures is presented in Table 2. The SSA was used to replace 20% and 35% of the mass of NA. The aggregate particle size distribution of the asphalt mixtures is shown in Figure 1, where the dashed lines represent the grading envelope, lower and upper limits, according to the Portuguese specifications [32]. Figure 2a shows the particles of the aggregate dimension 0/20 of SSA. Figure 2b presents the fraction of SSA dimension 11.2/16.0.

Table 2. Composition of the asphalt mixtures (% by mass).

Asphalt Mixture	NA	SSA	Filler	Bitumen
0% SSA	90.53	0.00	4.77	4.70
20% SSA	71.47	19.06	4.77	4.70
35% SSA	57.28	33.42	4.77	4.53

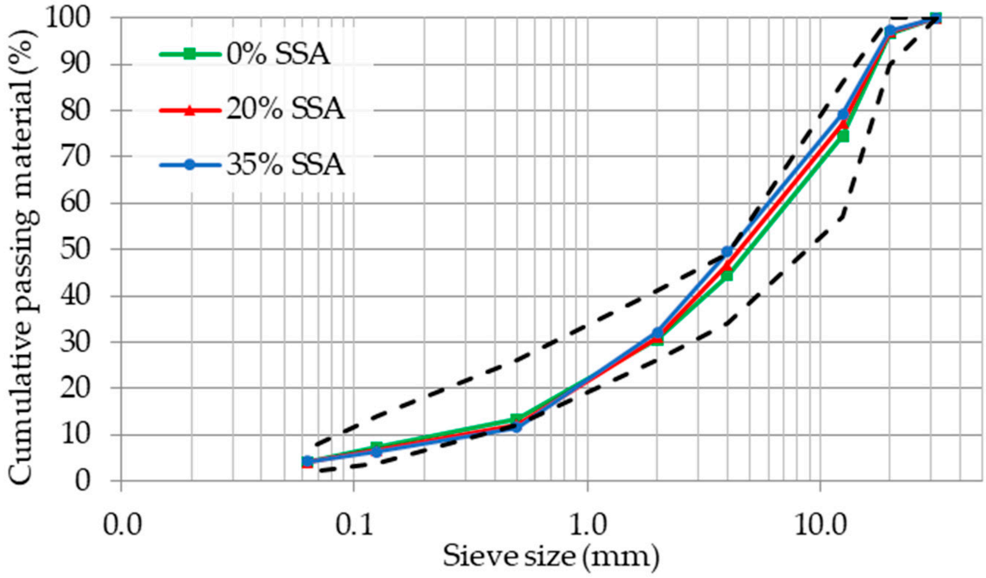

Figure 1. Particle size distribution of the asphalt mixtures.

(**a**) (**b**)

Figure 2. Particles of SSA: (**a**) fraction 0/20; (**b**) fraction 11.2/16.0.

The asphalt mixtures were compacted into cylindrical and prismatic specimens according to the required by the mechanical test to be performed. Cylindrical specimens (with 100 mm of diameter and 63.5 mm of height) were compacted by the impact compactor, following EN 12697-30 [33], applying 50 blows on each face. Cylindrical specimens were produced for the Marshall and water sensitivity tests. Prismatic specimens were compacted using the roller-compactor as described by EN 12697-33 [34]. In the case of the permanent deformation test, the specimens had the dimensions 400 mm × 300 mm × 60 mm. In the case of the fatigue resistance test, the compacted specimens had the dimensions 400 mm × 300 mm × 50 mm and were subsequently sawed into specimens with dimensions 400 mm × 50 mm × 50 mm. Figure 3a shows a prismatic specimen, and in Figure 3b can be observed the cutting face of a specimen for fatigue test. SSA particles are easily observed as shown in the image.

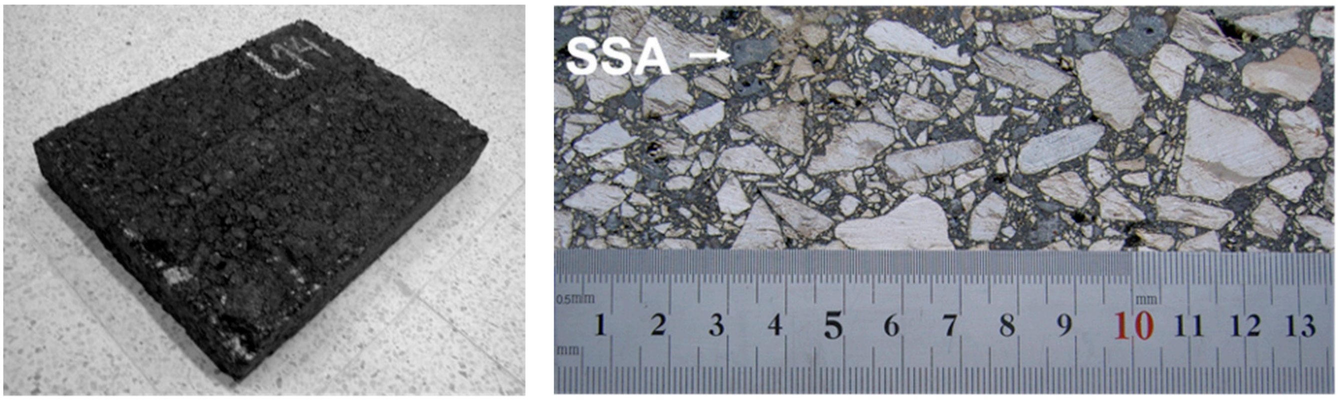

(**a**) (**b**)

Figure 3. Prismatic specimens: (**a**) general view; (**b**) detail of the cutting face.

2.2. Test Methods

An experimental program was developed to evaluate the effects of the incorporation of SSA in the performance of the asphalt mixtures. Firstly, the bonding between the binder (bitumen) and aggregate was evaluated through the affinity test, and following, the asphalt mixtures were tested to characterize the Marshall properties, fatigue resistance, permanent deformation, and water sensitivity. The test methods were selected according to European and Portuguese specifications [32].

The affinity between binder and aggregate was assessed through the rolling bottle method as described by EN 12697-11 [35]. The test consists of a visual evaluation of the degree of binder coverage on loose (uncompacted) binder-coated aggregates after a determined period of mechanical stirring in the presence of water. According to the test specification, the samples of aggregates were previously sieved, and only the fraction from 8 to 11.2 mm was used for the test. Bitumen was added to the aggregate and mixed until all surface of the aggregate particles were totally covered by bitumen. The amount of bitumen added was calculated, and corrected according to the respective aggregate density, to be 3.0% (by mass of mixture). After preparation and a resting period of 24 h, 150 g of the bitumen coated aggregates were transferred to the glass bottle previously filled with distilled water at 5 °C, a standardized glass rod was introduced in the bottle and the test was initiated. The affinity tests were conducted at a constant ambient temperature, 25 °C, and a fixed bottle rotation speed of 60 rpm. The degree of binder coverage of the aggregate particles was evaluated after 6 and 24 h of rotation. For each mixture, three tests (i.e., three individual bottles) were conducted.

The Marshall test, described in EN12697-34 [36], comprises the determination of stability, flow, and Marshall quotient (MQ). In this test, cylindrical specimens (100 mm diameter and 63.5 mm height) conditioned at 60 °C were placed in the Marshall test head and then loaded at a constant deformation rate of 50 mm/min until rupture. Prior to the Marshall test, the bulk density of each compacted specimen was determined according to EN12697-6 [37]. After the Marshall test, the specimens were disaggregated, and maximum density was determined according to EN12697-5 [38]. With these results other volumetric properties, namely voids content and voids in the mineral aggregate (VMA) were calculated as indicated in EN12697-8 [39].

Stiffness and fatigue resistance were evaluated by the four-point bending beam method as indicated by EN 12697-26—Annex B [40] and EN12697-24—Annex D [41], respectively. In these tests, the outer clamps of the equipment fix the prismatic specimen (400 mm × 50 mm × 50 mm) to the frame, allowing free rotation and horizontal translation, while the inner clamps apply a cyclic vertical load that induces a bending strain. All tests were carried out under strain-controlled conditions. The loading was applied in a sinusoidal configuration where load amplitude (bending strain), frequency, and temperature were kept constant during the test. In the case of fatigue tests, three strain levels were used. The selected strain levels were 150, 250, and 400 µm/m. Within each mixture, for each strain level, three specimens were tested. The loading frequency was 10 Hz and the test temperature was 20 °C. The criterion to terminate the test was a 50% reduction of the initial stiffness modulus. Before the fatigue tests, the stiffness tests were conducted under low strain, 50 µm/m, to avoid premature fatigue damage to the specimens. The stiffness was evaluated at 20 °C and for the loading frequencies of 1, 3, 5, 10, 20, and 30 Hz. A total of nine specimens per mixture were tested.

Permanent deformation was assessed through the wheel-tracking test. The tests were conducted following EN 12697-22 [42], using the wheel-tracking small size device, procedure B, and testing in air (dry conditions). During the test, a standardized moving wheel applied a vertical load of 700 N on the surface of the prismatic specimen (400 mm × 300 mm × 60 mm). The selected test temperature was 60 °C, as specified by the Portuguese specifications [31], and the test stopping criteria was reaching 20 mm of rut depth or 10,000 load cycles, whatever happens first. Per mixture, two specimens were tested.

To evaluate the water sensitivity, the indirect tensile strength (ITS) test was selected, as described in EN12697-23—method A [43]. In the ITS test, a diametrical compression load, at a constant rate of 50 mm/min, is applied to the cylindrical specimens until rupture occurs. The procedure to evaluate water sensitivity, as indicated in EN12697-12 [44], consisted in the determination of the ITS ratio (ITSR), which is computed as the ratio of the ITS of a group of specimens conditioned in water at 40 °C during approximately 70 h (ITS_{wet}) by the ITS of a group of unconditioned specimens (ITS_{dry}). After the wet/dry conditioning, the sets of test specimens were brought to the test temperature and conditioned for at least two hours. The selected test temperature was 15 °C as specified by the Portuguese specifications [31]. For each group (dry/wet), at least three individual specimens were tested.

3. Results and Discussion

3.1. Affinity between Aggregate and Binder

Figure 4 represents the evolution of the binder coverage of the aggregates during the affinity test. In this case, the limestone aggregate, which typically has a good affinity with bitumen, presented the best results. However, the SSA also exhibited good performance.

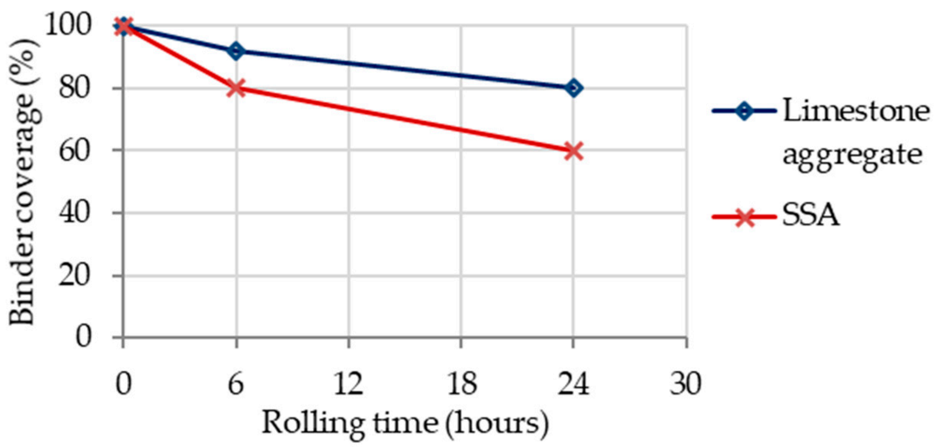

Figure 4. Evolution of the binder coverage of the aggregates during rolling time.

These results were in good agreement with the findings of other authors [45], that found the binder coverage of the aggregate, after 24 h and using the rolling bottle test, to be 75% in limestone aggregate, 40% in greywacke, 30% in basalt and 10% in granite. In a previous work [46], conducted by the same laboratory, the binder coverage of granitic aggregate was 73% and 40%, after 6 h and 24 h of rolling time, respectively. Thus, the SSA had better behavior than granite and worse than limestone. Generally, the affinity between aggregate and binder is driven by their chemical compatibility. Limestone is composed of calcium carbonate and magnesium carbonate, while granite is mainly composed of silica and alumina. Generally, the SSA is mainly composed of calcium oxide, silica, magnesium oxide, and alumina [31,47]. In the case of SSA, the presence of calcium oxide will induce some alkaline behavior that promotes adhesion with bitumen [48].

The performance of the aggregate in the affinity test can help to predict future problems for the asphalt pavement in service, e.g., its susceptibility to stripping. Thus, these results indicate no major concerns regarding the use of SSA in asphalt mixtures.

3.2. Marshall and Volumetric Properties

Table 3 presents the Marshall properties and other volumetric properties. Regarding stability, the values increased proportionally to the incorporation of SSA, closely following a linear trend. This might be explained by a better interlock promoted by the SSA particles. The flow also increased, however, the relation with SSA incorporation was not so clear. Consequently, an increase of the MQ can be observed as the incorporation of SSA increases.

Table 3. Marshall and volumetric properties.

Property	Asphalt Mixture		
	0% SSA	20% SSA	35% SSA
Binder content (% by mass)	4.70	4.70	4.53
Binder content (% by volume)	10.81	11.47	11.47
Stability (kN)	8.497	12.940	16.775
Flow (mm)	3.81	4.52	4.53
Marshall quotient (kN/mm)	2.2	3.0	4.0
Bulk density SSD (Mg/m^3)	2.377	2.526	2.626
Maximum density (Mg/m^3)	2.485	2.622	2.714
Air voids content (%)	4.34	3.64	3.26
Void in the mineral aggregate VMA (%)	15.18	15.17	15.20

As expected, the asphalt mixtures with SSA presented higher bulk and maximum densities due to the higher density of the SSA. The VMA was similar among all the asphalt mixtures and voids content was slightly lower in the asphalt mixtures with SSA. This difference was possibly the result of a small difference in the volumetric binder content. All the asphalt mixtures complied with the volumetric requirements (voids content from 3.0% to 6.0% and VMA minimum of 14%) set by the Portuguese specifications [31].

3.3. Stiffness and Fatigue Resistance

The results of the stiffness tests, stiffness modulus and phase angle, are presented in Figure 5, where the bars represent average values, and the error marks the respective standard deviation. As expected, the increase of the loading frequency caused an increase of the stiffness modulus and a decrease of phase angle. In general, the behavior of all the studied asphalt mixtures was similar, highlighted by a visual overlap of the error marks.

Generally, the stiffness of the asphalt mixture is highly dependent on the type of bitumen and binder content. If these variables remain unchanged, as well as the mixture type and compaction conditions (i.e., voids content), one can expect similar stiffness results. Furthermore, the percentages of aggregate substitution (20% and 35%) are moderate, thus a significant change in behavior is not to be expected. The differences observed in the stiffness results can be explained by the production (specimen mixing and compaction) and experimental variability.

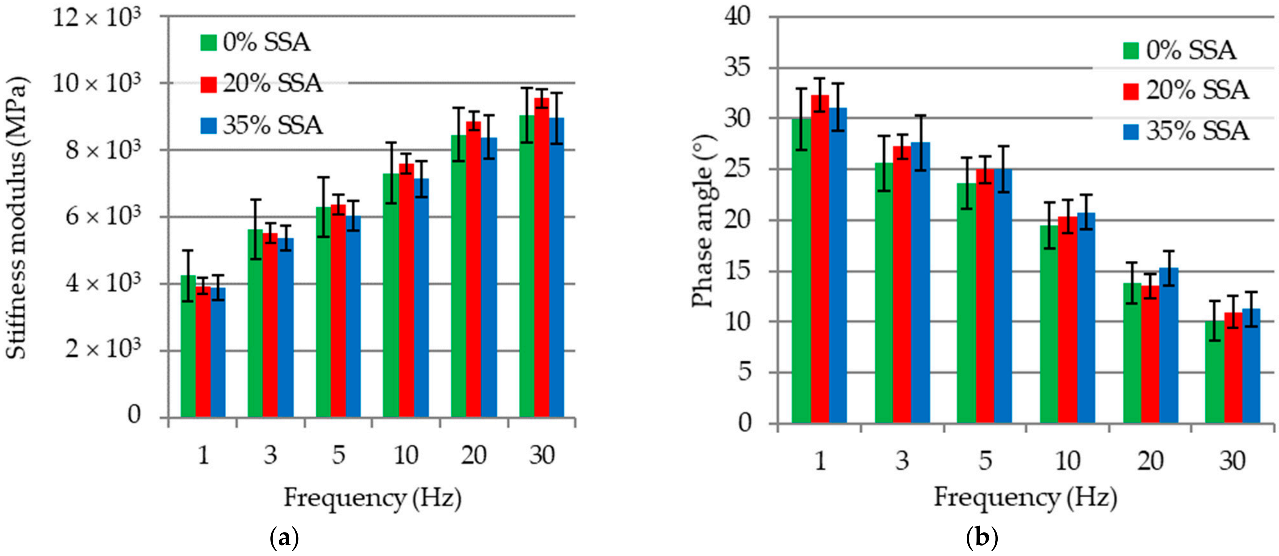

Figure 5. (**a**) Stiffness modulus; (**b**) phase angle.

The result of the fatigue resistance test, for each tested specimen, was the number of cycles (fatigue life) for the respective loading strain being applied. The individual test results were used to derive fatigue lines. Figure 6 presents the obtained fatigue lines, where it can be observed that the incorporation of SSA was not detrimental to the fatigue resistance of the asphalt mixture.

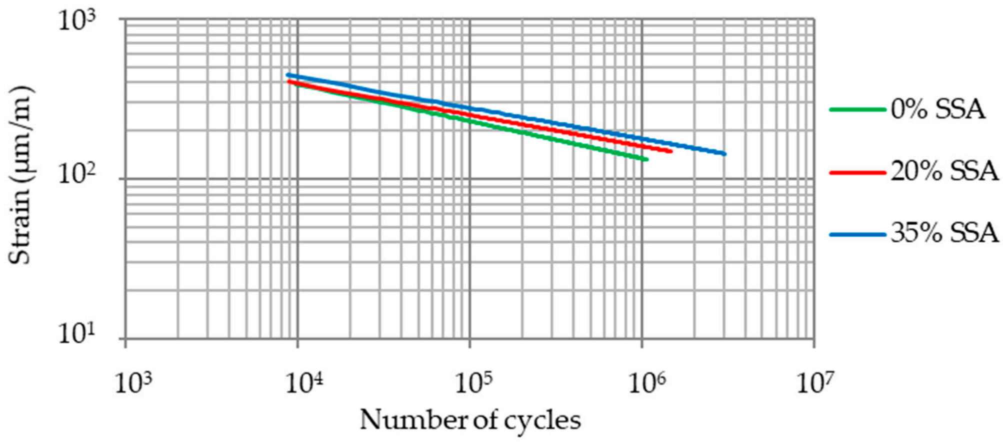

Figure 6. Fatigue lines.

The fatigue lines can be written according to the following equation:

$$\log(N) = A_0 + A_1 \times \log(\varepsilon) \quad (1)$$

where: N is the fatigue life (number of cycles to reach the failure criterion), ε is the applied loading strain, A_0 and A_1 are constants (determined by linear regression in the log-log space). When plotted in a log-log space, A_1 corresponds to the slope of the fatigue line. Table 4 presents the parameters determined for the fatigue lines, ε_6 (strain correspondent to fatigue life of one million cycles) and R^2 (coefficient of determination).

Regarding fatigue resistance, the behavior among the asphalt mixtures can be considered approximately similar. The asphalt mixtures with SSA performed slightly better than the reference mixture. However, this can be partially explained by the variability of this type of test and a small difference in the volumetric binder content, which is a bit higher in the case of SSA asphalt mixtures (Table 3).

Table 4. Parameters of the fatigue lines.

Asphalt Mixture	A_0	A_1	ε_6 (µm/m)	R^2
0% SSA	15.122	−4.292	134	0.981
20% SSA	17.302	−5.128	160	0.994
35% SSA	17.677	−5.181	179	0.936

3.4. Permanent Deformation

The main results of the wheel-tracking test were the proportional rut depth (PRD) and the wheel-tracking slope (WTS). Figure 7 presents the evolution of the PRD during the test for the two specimens of each mixture type, according to the standard test [41]. Table 5 presents the PRD and WTS obtained at the end of the test (10,000 load cycles).

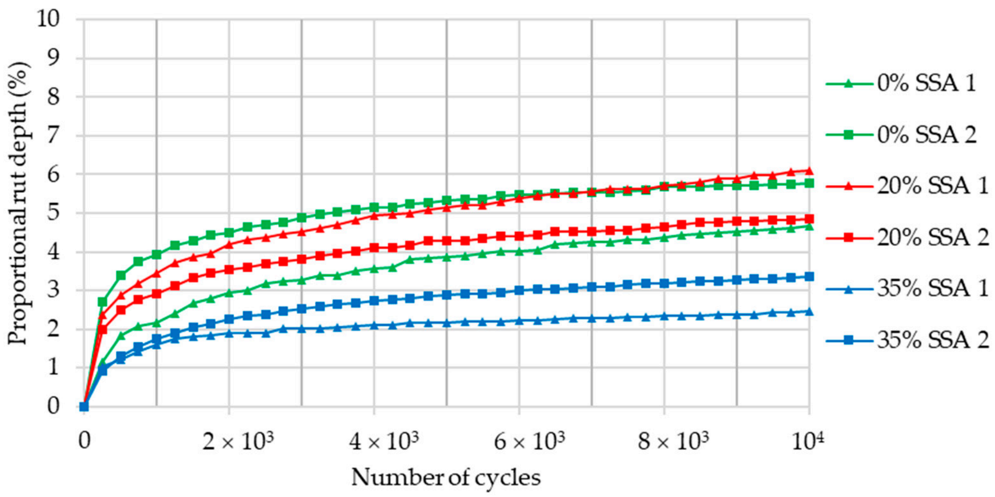

Figure 7. Evolution of the proportional rut depth during the wheel-tracking tests.

Table 5. Results of the wheel-tracking test.

Asphalt Mixture	Specimen	PRD_{AIR} (%)		WTS_{AIR} (mm/10^3 Cycles)	
0% SSA	1	4.7	5.2	0.098	0.077
	2	5.8		0.056	
20% SSA	1	6.1	5.5	0.116	0.092
	2	4.8		0.068	
35% SSA	1	2.5	2.9	0.034	0.046
	2	3.4		0.058	

The tests were terminated by the stopping criteria of the 10,000 load cycles (Figure 7). Considering that the specimens had a thickness of approximately 60 mm, for the stopping criteria of the 20 mm rut depth the PRD would need to be near 33%. In this study, the PRD values were lower and comprised between 2.5 and 6.1% (Table 5). The values of WTS were in the interval of 0.034 and 0.116 mm/10^3 cycles (Table 5).

All the test results corroborated that the asphalt mixtures exhibited a good performance against permanent deformation. The incorporation of SSA has not affected this good behavior as expected. In particular, the asphalt mixture with 35% SSA performed slightly better than the previous asphalt mixtures, possibly due to a better aggregate interlock promoted by the higher quantity of SSA. In principle, the incorporation of SSA, ensuring the good design of the asphalt mixture, will always tend to at least preserve or even increase the resistance to permanent deformation.

3.5. Water Sensitivity

Figure 8 presents the results of ITS_{dry} and ITS_{wet} as well as the standard deviation for each category. In Figure 8 it is also indicated the respective ITSR for each case study. In general, water affected the aggregate-binder bonding leading to a reduction of ITS. Thus, the higher the ITSR, the better the mixture.

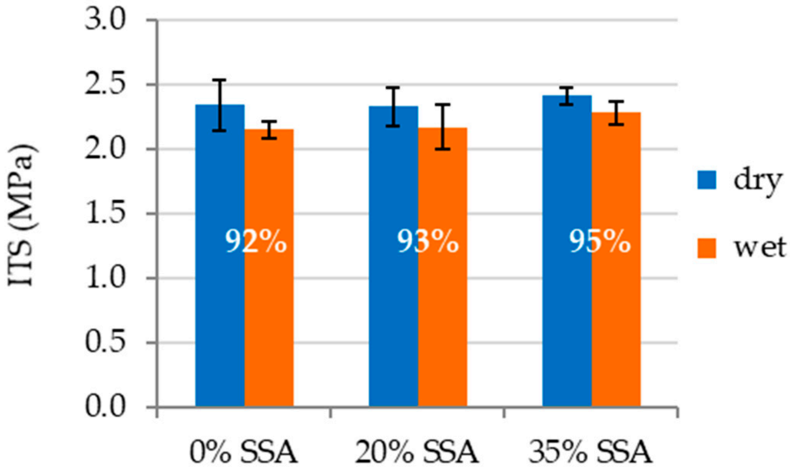

Figure 8. Average values of ITS, standard deviation and ITSR.

The ITS and ITSR results indicated a similar performance among all the asphalt mixtures, highlighting that the incorporation of SSA did not compromise the good performance of the mixture. However marginally, the mixture with 35% SSA had the best results.

Worth mentioning that the limestone aggregate has a particularly good affinity with the binder, which usually corresponds to high ITSR values. The technical requirements [31] indicate a minimum ITSR of 80%. In this case, all the asphalt mixtures complied with the specification.

4. Conclusions

The mechanical performance of asphalt mixtures with the incorporation of steel slag aggregate (SSA) was evaluated through a dedicated experimental program. To replace the natural aggregate, two incorporation rates of SSA were studied, 20% and 35%. Also, one reference mixture was considered (0% SSA). The asphalt mixtures were tested, in the laboratory, for affinity between aggregate and binder, Marshall and volumetric properties, stiffness, fatigue resistance, permanent deformation, and water sensitivity.

Regarding the incorporation of SSA in asphalt mixtures, the evaluation of mechanical performance indicated that the SSA can perform approximately equally to good quality natural aggregates. In the case of Marshall stability, the incorporation of SSA had a clear effect in increasing stability. In other cases, such as permanent deformation and water sensitivity, SSA may have some positive effects. However, in these cases, the contributions were marginal.

The experimental program highlights the suitability of the application of SSA in pavement layers. The construction of pavement layers is an activity that consumes high quantities of materials. Thus, the use of SSA in such a large-scale application will bring added value to an industrial waste, as well as promote a reduction in the extraction of non-renewable natural resources.

Author Contributions: Conceptualization, J.N.; methodology, J.N. and J.C.; formal analysis, J.N. and J.C.; investigation, J.N. and J.C.; data curation, J.C.; writing—original draft preparation, J.N.; writing—review and editing, J.N. and J.C.; supervision, J.N. All authors have read and agreed to the published version of the manuscript.

Funding: This research received no external funding.

Acknowledgments: This work is part of the research activity carried out at Civil Engineering Research and Innovation for Sustainability (CERIS) and has been funded by Fundação para a Ciência e a Tecnologia (FCT) in the framework of project UIDB/04625/2020. The authors acknowledge the Laboratory of Transportation Infrastructures of the Department of Civil Engineering, Architecture and Georesourses, Instituto Superior Técnico, University of Lisbon, for carrying out the tests. An acknowledgment is addressed to the Harsco company for supplying the SSA used in the experimental study.

Conflicts of Interest: The authors declare no conflict of interest.

References

1. Bamigboye, G.; Bassey, D.; Olukanni, D.; Ngene, B.; Adegoke, D.; Odetoyan, A.; Kareem, M.; Enabulele, D.; Nworgu, A. Waste materials in highway applications: An overview on generation and utilization implications on sustainability. *J. Clean. Prod.* **2021**, *283*, 124581. [CrossRef]
2. Gomes Correia, A.; Winter, M.G.; Puppala, A.J. A review of sustainable approaches in transport infrastructure geotechnics. *Transp. Geotech.* **2016**, *7*, 21–28. [CrossRef]
3. Euroslag (The European Association Representing Metallurgical Slag Producers and Processors). Statistics 2018, 2022. Germany. Available online: https://www.euroslag.com/wp-content/uploads/2022/04/Statistics-2018.pdf (accessed on 1 November 2022).
4. FHWA (Federal Highway Administration). User Guidelines for Waste and Byproduct Materials in Pavement Construction. Publication Number: FHWA-RD-97-148; 2022. Available online: https://www.fhwa.dot.gov/publications/research/infrastructure/structures/97148/ssa1.cfm (accessed on 1 November 2022).
5. CEN. *EN 13242+A1—Aggregates for Unbound and Hydraulically Bound Materials for Use in Civil Engineering Work and Road Construction*; European Committee for Standardization: Brussels, Belgium, 2007.
6. Correia, A.G.; Roque, A.J.; Ferreira, S.M.R.; Fortunato, E. Case Study to Promote the Use of Industrial Byproducts: The Relevance of Performance Tests. *J. ASTM Int.* **2012**, *9*, 1–18.
7. Piatak, N.; Parsons, M.; Seal, R., II. Characteristics and environmental aspects of slag: A review. *Appl. Geochem.* **2015**, *57*, 36–266. [CrossRef]
8. Skaf, M.; Manso, J.; Aragón, A.; Fuente-Alonso, J.; Ortega-López, V. EAF slag in asphalt mixes: A brief review of its possible re-use. *Resour. Conserv. Recycl.* **2017**, *120*, 176–185. [CrossRef]
9. Sorlini, S.; Sanzeni, A.; Rondi, L. Reuse of steel slag in bituminous paving mixtures. *J. Hazard. Mater.* **2012**, *209–210*, 84–91. [CrossRef] [PubMed]
10. Gokalp, I.; Uz, V.; Saltan, M.; Tutumluer, E. Technical and environmental evaluation of metallurgical slags as aggregate for sustainable pavement layer applications. *Transp. Geotech.* **2018**, *14*, 61–69. [CrossRef]
11. Loureiro, C.D.A.; Moura, C.F.N.; Rodrigues, M.; Martinho, F.C.G.; Silva, H.M.R.D.; Oliveira, J.R.M. Steel slag and recycled Concrete aggregates: Replacing quarries to supply sustainable materials for the asphalt paving industry. *Sustainability* **2022**, *14*, 5022. [CrossRef]
12. Gulisano, F.; Crucho, J.; Gallego, J.; Picado-Santos, L. Microwave Healing Performance of Asphalt Mixture Containing Electric Arc Furnace (EAF) Slag and Graphene Nanoplatelets (GNPs). *Appl. Sci.* **2020**, *10*, 1428. [CrossRef]
13. Gulisano, F.; Buasiri, T.; Apaza, F.; Cwirzen, A.; Gallego, J. Piezoresistive Behavior of Electric Arc Furnace Slag and Graphene Nanoplatelets Asphalt Mixtures for Self-Sensing Pavements. *Autom. Constr.* **2022**, *142*, 104534. [CrossRef]
14. Jiao, W.; Sha, A.; Liu, Z.; Jiang, W.; Hu, L.; Li, X. Utilization of steel slags to produce thermal conductive asphalt concretes for snow melting pavements. *J. Clean. Prod.* **2020**, *261*, 121197. [CrossRef]
15. Ameri, M.; Hesami, S.; Goli, H. Laboratory evaluation of warm mix asphalt mixtures containing electric arc furnace (EAF) steel slag. *Constr. Build. Mater.* **2013**, *49*, 611–617. [CrossRef]
16. Chen, Z.; Wu, S.; Wen, J.; Zhao, M.; Yi, M.; Wan, J. Utilization of gneiss coarse aggregate and steel slag fine aggregate in asphalt mixture. *Constr. Build. Mater.* **2015**, *93*, 911–918. [CrossRef]
17. Chen, Z.; Leng, Z.; Jiao, Y.; Xu, F.; Lin, J.; Wang, H.; Cai, J.; Zhu, L.; Zhang, N.; Dong, Y.; et al. Innovative use of industrially produced steel slag powders in asphalt mixture to replace mineral fillers. *J. Clean. Prod.* **2022**, *344*, 131124. [CrossRef]
18. Fakri, M.; Ahmadi, A. Recycling of RAP and steel slag aggregates into the warm mix asphalt: A performance evaluation. *Constr. Build. Mater.* **2017**, *147*, 630–638. [CrossRef]
19. Fakri, M.; Ahmadi, A. Evaluation of fracture resistance of asphalt mixes involving steel slag and RAP: Susceptibility to aging level and freeze and thaw cycles. *Constr. Build. Mater.* **2017**, *157*, 748–756. [CrossRef]
20. Martinho, F.; Picado-Santos, L.; Capitão, S. Influence of recycled concrete and steel slag aggregates on warm-mix asphalt properties. *Constr. Build. Mater.* **2018**, *285*, 684–696. [CrossRef]
21. Massoudi, S.; Abtahi, S.; Goli, A. Evaluation of electric arc furnace steel slag coarse aggregate in warm mix asphalt subjected to long-term aging. *Constr. Build. Mater.* **2017**, *135*, 260–266. [CrossRef]
22. Zhao, X.; Sheng, Y.; Lv, H.; Jia, H.; Liu, Q.; Ji, X.; Xiong, R.; Meng, J. Laboratory investigation on road performances of asphalt mixtures using steel slag and granite as aggregate. *Constr. Build. Mater.* **2022**, *315*, 125655. [CrossRef]

23. Chen, J.; Wei, S. Engineering properties and performance of asphalt mixtures incorporating steel slag. *Constr. Build. Mater.* **2016**, *128*, 148–153. [CrossRef]
24. Goli, A. The study of the feasibility of using recycled steel slag aggregate in hot mix asphalt. *Case Stud. Constr. Mater.* **2022**, *16*, e00861. [CrossRef]
25. Neves, J.; Crucho, J.; Picado Santos, L.; Martinho, F. The influence of processed steel slag on the performance of a bituminous mixture. In Proceedings of the Ninth International Conference on Bearing Capacity of Roads, Railways and Airfields, Trondhein, Norway, 25–27 June 2013; pp. 617–625.
26. Pasetto, M.; Baldo, N. Mix design and performance analysis of asphalt concretes with electric arc furnace slag. *Constr. Build. Mater.* **2011**, *25*, 3458–3468. [CrossRef]
27. Xie, J.; Chen, J.; Wu, S.; Lin, J.; Wei, W. Performance characteristics of asphalt mixture with basic oxygen furnace slag. *Constr. Build. Mater.* **2013**, *38*, 796–803. [CrossRef]
28. Xie, J.; Wu, S.; Lin, J.; Cai, J.; Chen, Z.; Wei, W. Recycling of basic oxygen furnace slag in asphalt mixture: Material characterization & moisture damage investigation. *Constr. Build. Mater.* **2012**, *36*, 467–474.
29. Xie, J.; Wu, S.; Zhang, L.; Xiao, Y.; Liu, Q.; Yang, C.; Nie, S. Material characterization and performance evaluation of asphalt mixture incorporating basic oxygen furnace slag (BOF) sludge. *Constr. Build. Mater.* **2017**, *147*, 362–370. [CrossRef]
30. Alves, R.; Rios, S.; Fortunato, E.; Viana da Fonseca, A. Mechanical Behaviour of Steel Slag-Rubber Mixtures: Laboratory Assessment. *Sustainability* **2023**, *15*, 1563. [CrossRef]
31. Martinho, F.; Picado-Santos, L.; Capitão, S. Feasibility Assessment of the Use of Recycled Aggregates for Asphalt Mixtures. *Sustainability* **2018**, *10*, 1737. [CrossRef]
32. IP. *Specifications*; Portuguese Infrastructure Agency: Almada, Portugal, 2014.
33. *EN 12697-30*; Bituminous Mixtures—Test Methods for Hot Mix Asphalt—Part 30: Specimen Prepared by Impact Compactor. European Committee for Standardization: Brussels, Belgium, 2012.
34. *EN 12697-33*; Bituminous Mixtures—Test Methods for Hot Mix Asphalt—Part 33: Specimen Prepared by Roller Compactor. European Committee for Standardization: Brussels, Belgium, 2019.
35. *EN 12697-11*; Bituminous Mixtures—Test Methods for Hot Mix Asphalt—Part 11: Determination of the Affinity between Aggregate and Bitumen. European Committee for Standardization: Brussels, Belgium, 2020.
36. *EN 12697-34*; Bituminous Mixtures—Test Methods for Hot Mix Asphalt—Part 34: Marshall Test. European Committee for Standardization: Brussels, Belgium, 2007.
37. *EN 12697-6*; Bituminous Mixtures—Test Methods for Hot Mix Asphalt—Part 6: Determination of Bulk Density of Bituminous Specimens. European Committee for Standardization: Brussels, Belgium, 2020.
38. *EN 12697-5*; Bituminous Mixtures—Test Methods for Hot Mix Asphalt—Part 5: Determination of the Maximum Density. European Committee for Standardization: Brussels, Belgium, 2017.
39. *EN 12697-8*; Bituminous Mixtures—Test Methods for Hot Mix Asphalt—Part 8: Determination of Void Characteristics of Bituminous Specimens. European Committee for Standardization: Brussels, Belgium, 2018.
40. *EN 12697-26*; Bituminous Mixtures—Test Methods for Hot Mix Asphalt—Part 26: Stiffness. European Committee for Standardization: Brussels, Belgium, 2018.
41. *EN 12697-24*; Bituminous Mixtures—Test Methods for Hot Mix Asphalt—Part 24: Resistance to Fatigue. European Committee for Standardization: Brussels, Belgium, 2018.
42. *EN 12697-22*; Bituminous Mixtures—Test Methods for Hot Mix Asphalt—Part 22: Wheel Tracking. European Committee for Standardization: Brussels, Belgium, 2020.
43. *EN 12697-23*; Bituminous Mixtures—Test Methods for Hot Mix Asphalt—Part 23: Determination of the Indirect Tensile Strength of Bituminous Specimens. European Committee for Standardization: Brussels, Belgium, 2017.
44. *EN 12697-12*; Bituminous Mixtures—Test Methods for Hot Mix Asphalt—Part 12: Determination of the Water Sensitivity of Bituminous Specimens. European Committee for Standardization: Brussels, Belgium, 2018.
45. Porot, L.; Soenen, H.; Apeagyei, A.; Grenfell, J.; Vansteenkiste, S.; Chailleux, E. Recommendation of RILEM TC 237-SIB on affinity between aggregates and bituminous binders. *Mater. Struct.* **2018**, *51*, 173. [CrossRef]
46. Crucho, J.; Neves, J.; Capitão, S.; Picado-Santos, L. Mechanical performance of asphalt concrete modified with nanoparticles: Nanosilica, zero-valent iron and nanoclay. *Constr. Build. Mater.* **2018**, *181*, 309–318. [CrossRef]
47. Nicula, L.; Corbu, O.; Iliescu, M.; Dumitras, D. Using the blast furnace slag as alternative source in mixtures for the road concrete for a more sustainable and a cleaner environment. *Rom. J. Mater.* **2020**, *50*, 545–555.
48. Li, C.; Chen, Z.; Wu, S.; Li, B.; Xie, J.; Xiao, Y. Effects of steel slag fillers on the rheological properties of asphalt mastic. *Constr. Build. Mater.* **2017**, *145*, 383–391. [CrossRef]